DOI: 10.1177/0003702820960737

Paper Type: *Submitted Paper*

Odorant Monitoring in Natural Gas Pipelines Using Ultraviolet–Visible Spectroscopy

Rossana Galassi,[1]* Christian Contini,[2] Matteo Pucci,[2] Ennio Gambi,[3] Gabriele Manca[4]

[1]University of Camerino, School of Science and Technology, Chemistry Division, Via Sant'Agostino, 1, Camerino, I-62032, Italy

[2]Automa srl, Via Casine di Paterno 122/A, 60019 Ancona

[3]Università Politecnica delle Marche, Dipartimento di Ingegneria dell'Informazione–Via Brecce Bianche 12, I-60131 Ancona,

[4]Istituto di Chimica dei Composti Organo-Metallici, ICCOM-CNR, Via Madonna del Piano 10, I-50019 Sesto Fiorentino, Italy

*Corresponding author email: rossana.galassi@unicam.it

Abstract

The remote, timely and in-field detection of sulfured additives in natural gas pipelines is a challenge for environmental, commercial and safety reasons. Moreover, the constant control of the level of odorants in a pipeline is required by law to prevent explosions and accidents. Currently, the detection of the most common odorants (THT = thiophane, and TBM = tertiary butyl mercaptan) added to natural gas streams in pipelines is made in situ by using portable gas chromatography (CG) apparatuses. In this study, we report the analysis of the ultraviolet (UV) spectra obtained by a customized UV spectrophotometer, named Spectra, for the in-field detection of THT and TBM. Spectra was conceived to accomplish the remote analysis of odorants in the pipelines of the natural gas stream through the adoption of technical solutions aimed to adapt a basic bench UV spectrophotometer to the in-field analysis of gases. The remotely controlled system acquires spectra continuously, performing the quantitative determination of odorants and catching systemic or accidental variations of the gaseous mixture in different sites of the pipeline. The analysis of the experimental spectra was carried out also through theoretical quantum mechanical approach aimed to detect and to correctly assign the nature of the intrinsic electronic transitions of the two odorants, THT and TBM, that cause the

DOI: 10.1177/0003702820960737

UV absorptions. So far, these theoretical aspects have never been studied before. The absorption maxima of THT and TBM spectra were computationally simulated through the usage of selected molecular models with satisfactory results. The good matches between the experimental and theoretical datasets corroborate the reliability of the collected data. During the tests, also unexpected pollutants and accidental malfunctions have been detected and also identified by Spectra, making this instrument suitable for many purposes.

Keywords: Portable ultraviolet spectrophotometer, natural gas odorants, field detection, thiphane, THT detection, vibronic structure, time-dependent density functional theory calculations, TD-DFT

Introduction

Natural gas is an odorless, colorless and flammable gas worldwide spread for civil uses.[1] For safety requirements, suitable odorants are added in order to detect the presence of gas in air in concentrations below the lower explosive limit (LEL); besides the unpleasant smell, the odorant addition must not change the physical or chemical properties of natural gas. Most common odorizing agents are linear or branched chain aliphatic sulfides such as ethyl mercaptan, dimethylsulfide (DMS), isopropyl mercaptan (IPM), tertiary butyl mercaptan (TBM), normal propyl mercaptan (NPM), methyl ethyl sulfide (MES), secondary butyl mercaptan (SBM) or cyclic such as thiophane (THT).[2] In Europe the most common odorizing agent is the THT, which is known not to be easily oxidized or to have low odor impact that is at least not as pungent as TB, and exhibits poor soil penetration; it is usually used either as pure or in blends such as 50% THT with 50% TBM.[2] There are many issues to take in consideration to set up the odorization of natural gas such as (i) the odor intensity of the selected odorant,[3] (ii) the maintenance of its minimum concentration in gas,[3] (iii) the choice of the device for the odorant's detection according to these standards,[2] given that a precise measurement of the concentration of the odorant is required mainly for civil safety but also for financial concerns. The demand to prevent unnecessary overloads of sulfur based odorants in natural gas is also related to environmental issues, as the combustion of odorized gas leads to the unavoidable production of pollutants that cause acid rains and other environmental consequences.[1–4] This latter aspect puts the base for other additional needs, such as the constant and continuous control of odorant levels to avoid injecting exceeding amounts of THT or TBM. Efficient online analyses of natural gas streams

DOI: 10.1177/0003702820960737

are highly desirable and, currently, these are mainly based on chromatographic methods,[5] with all the limits and worries of this technique that, even suitable and reliable, is surely limited by technical concerns and high procedural costs.[6] Many studies have been addressed to the challenging purpose of detecting and monitoring gaseous mixtures according to both chromatographic,[7,8] as well as to spectroscopic methods.[9,10] In particular, the recent development of portable gas chromatography (GC) systems created by the integration of micro fabricated components makes these tools suitable for rapid and on-site analysis of a number of complex chemical mixtures, including natural gas streams in pipelines.[11] Portable gas chromatography (GC) systems, also equipped with mass analyzers,[12] may be set up for the measurements of THT (5 ppm) or TBM (1–3 ppm range) directly in the pipeline with an accuracy and a precision of analysis in the range of bench-top instruments. Portable GCs afford to a shortening of the analysis' time by avoiding the in-field sampling and the further delivery of the samples to remote laboratories. Currently, GC measurements are the most used and recognized as reliable for the detection of odorizing agents in natural gas.[13,14] However, the use of this instrumentation with an automatized sampler and a permanent, continuous analyzer of the gaseous mixture stream directly in-field involves a series of problems, as in example, the constant need of a carrier gas, the maintenance of the columns and the operating conditions, whose variation due to climatic effects can cause the alteration of the measurement.[6] By considering these issues, alternative analytical methods have been taken into account with further attention being drawn on spectroscopic methods. With the aim to develop a prototype for on-line measurements, we present here a novel approach to the TBM and THT detection in odorized natural gas. In particular, we investigated the application of a customized UV–visible (UV–Vis) spectrophotometer instrument in the detection and in the quantification of the two mentioned odorants, when they are dispersed in real matrices of natural gas that flow through pipelines. The acquired UV spectra, examined by both direct absorptiometry and a multiwavelength approach, were collected to serve as a database for the aforementioned applicative purposes. To clarify the relevance of the data, the definition of their electronic nature was studied using quantum mechanical techniques. The combination of the theoretical and experimental approaches supports the prototype herein proposed and puts the bases for its use in the quantitative determination of odorants in natural gas in the ppm range of concentration.

DOI: 10.1177/0003702820960737

UV–Vis Spectral Analysis

Background

The most commonly used measurement technique in the detection of complex gaseous mixtures, so far, is the combination of gas chromatography (GC) with either a flame ionization detector (FID), mass spectroscopy[15] or in combination with an array of highly integrated and selective metal oxide (MOX) sensors.[16] However, the development of the UV spectrophotometry in the analysis of gas mixtures has prompted us to adopt this fast technique for the measurements of odorants.[17,18] In the first place, in comparison with other optical methods, this technology presents some important features such as the ease and robustness of the optical technique and the analysis of low concentration range (from 10^{-3} to thousands mg/m^3).[19] Furthermore, methane, which is the largest component of natural gas, exhibits UV absorptions up to 140 nm,[20] as well as propane[21] and ethane, which exhibit a characteristic serrated band of absorption up to 150 nm.[20–22] Conversely, sulfur compounds adsorb UV light in the spectral region above 195 nm.[23] Moreover, UV spectral examination may be performed by direct absorptiometry or by means of a multiwavelength approach. In the former method, a single wavelength is used; hence, by knowing absorbance values at given concentrations of a species, it is easy to determine an unknown concentration of the same species; therefore, the selection of a characteristic wavelength must be carried out for the studied compound. In the multiwavelength approach, the analysis is based on spectral deconvolution, a classical multicomponent analysis carried out by using a deterministic approach which simultaneously evaluates the contributions of each species by computational and chemometric methods.[24,25]

Materials

All analytical gas samples for the in house analysis were obtained from Risam Gas with a concentration ranging from 10 to 50 mg/Sm^3 in either Nitrogen or Methane. In-field gas samples were spilled directly from medium-pressure (3–5 bar) distribution pipelines with the consent of the distributors.

Instrumentation

Ultraviolet–visible spectra were acquired using a custom-built UV–Vis spectrophotometer prototype (later named Spectra). The optical path of the instrument consists of a UV deuterium

DOI: 10.1177/0003702820960737

lamp, a custom stainless steel flow cell with built-in focusing lenses, a commercial UV spectrophotometer and two optical fibers with a 600 µm quartz core. The spectrophotometer is capable of analyzing light in the 180–450 nm wavelength range, but the measuring range was limited to 200–280 nm (unless otherwise specified) to obtain the best possible resolution over the wavelengths of interest. The instrument includes a particulate filter, a pressure reducer, valves, and pumps to control the gas flow through the cell. Every component is controlled by proprietary electronics. Validation of the measurements made with Spectra on the pipelines was carried out by comparing them with the results of the GC analysis in different pipelines and with those obtained by Spectra on standard canisters at known concentrations (normed according to ISO 6143). The prototype system is currently patent pending.

Spectra Acquisition Method

During the analyses, every analytical gas sample was kept at 2 bar pressure and at room temperature. The technical steps needed for each measurement may be summarized as follows: Each procedure starts with a systematic process of cleaning of the gas cell, followed by the introduction of the reference gas, a reading of the light transmitted through the reference gas (blank), the introduction of the odorized natural gas and another reading of the light transmitted (sample). Each reading is performed after letting the gas stabilize inside the gas cell. Each spectrum consists of the average of 50 subsequent 0.1 s acquisitions. No other mathematical pre-processing is performed. Direct absorptiometry of THT was performed by comparing the absorbance of the gas mixture at 230 nm with the absorption of THT/methane standard canisters at the same wavelength.

The method of analysis is based on the well-known Beer–Lambert Law, where the experimental absorbance of a gas sample is calculated by considering a reference gas as blank:

$$A_{experimental} = A_{sample} - A_{blank} = -\log\frac{I_{sample}}{I_{blank}} \quad (1)$$

If the reference gas is non-absorbing in the range of interest (200–280 nm), $A_{experimental}$ corresponds to A_{sample}. Conversely, if the reference gas shows absorptions in the observed range, the attained spectrum might display negative bands, according to Eq. 1. Consequently, the choice of the reference gas is fundamental for this method of analysis. In this regard, the gas in pipelines is mainly composed by a mixture of light hydrocarbons consisting of 90–95% of methane.

DOI: 10.1177/0003702820960737

Methane and other light aliphatic hydrocarbons do not show absorptions in the range of analysis chosen for the herein described purposes, therefore they might be used as reference gases; however, the acquisition of a blank measurement with a hydrocarbon matrix poses major problems for an in-field automated measuring system, because it implies the use of canisters of combustible gas in unsupervised environments, bringing up safety concerns and the need for frequent replacement of the hydrocarbon canisters. An alternative non absorbing gas to methane might be nitrogen, being safe and available in canisters; moreover, in the range 200–280 nm, no significant differences between spectra of a standard odorant–methane mixture and spectra of a standard odorant–nitrogen mixture were observed in laboratory trials. Using nitrogen would rule out the concerns arising from the use of combustible gas, but it would still defeat the whole purpose of achieving an in-field automated and independent machine because of the need of maintenance and replacement of the canisters. The concerns were removed by using atmospheric air. Atmospheric air does not show significant absorptions at wavelengths higher than 200 nm hence it represents a cheap and readily available reference gas to set up Spectra for the in-field analysis. In summary, above 200 nm, methane, nitrogen, and air appear to be equivalent as reference gases with regard to Eq. 1, but the choice of air allows the instrument to be completely independent. Since air was chosen as the reference gas, its characteristic absorptions (see Figure S1, Supplemental Material), attributed to the absorption of oxygen,[26] may appear as negative peaks below 200 nm in the resulting spectra. In the same way, the occasional presence of unexpected UV-active pollutants in air, whose absorptions are in the range of interest, may originate negative bands in the final spectra. Nevertheless, the negative peaks due to oxygen do not affect the measurements because of the substantial wavelength difference between oxygen and odorant absorptions; in contrast, absorptions due to occasional pollutants in the reference gas might definitely interfere with the odorant measurements. This problem was observed in a specific booth placed near a polystyrene manufacturing industry; natural gas spectra acquired in that booth occasionally showed a large negative band centered at 235 nm that was tentatively assigned to styrene according to data reported in the literature.[27] In practice, the issue was tackled by automatically checking every spectrum for unexpected signals, by discarding the faulty measurements and by triggering alerts for the user.

UV–Visible Spectral Analysis of THT and TBM

DOI: 10.1177/0003702820960737

UV–Visible Spectra

The UV–Vis spectra of gaseous THT and TBM were recorded with Spectra in methane in different concentrations that averaged ~45 mg/Sm^3 and ~18 mg/Sm^3, respectively (corresponding to 0.00125%–0.0005% of odorant). The ultraviolet absorption spectrum of CH_4 consists of a continuous absorption with two diffuse broad peaks in the 8.8–11.4 eV photon energy range assigned to Rydberg transitions,[28–30] whereas the absorption spectrum of ethane (C_2H_6) shows considerable vibronic structures.[29] Light alkanes, the largest components of natural gas, absorb in a UV region quite below 200 nm resulting suitable as dispersive medium for UV absorption analysis of sulfur containing compounds whose absorptions fall at higher wavelengths.[31] The absorption profiles recorded for THT and TBM with Spectra on standard canisters at room temperature are reported in Figure 1 and their appearance is quite characteristic.

An interpretation of the absorption spectrum of THT shown in Figure 1 was attempted on the basis of the data reported in the literature.[23] In the literature, the maxima for a not fully specified $(CH_2)_4S$ compound are reported at 210 and 239 nm in ethanol solution. These data are comparable with those obtained by Tarbell and Weaver for an ambiguous related sulfur compound.[32] In the spectrum shown in Figure 1, a quite intense serrated curve is observed with a maximum absorption at 209 nm attributable to a likely vibronic structure with peaks separation of 2.6–2.9 nm. The curve intensity falls at 211 nm and another less intense but broader asymmetric band appears at about 228 nm.

The spectrum obtained for TBM, shown in Figure 1, consists of a wide absorption band with a maximum at 204 nm, and a very broad and flattened band centered at about 230 nm, which ends with a tail around 260 nm. By comparing with the THT spectrum we observe a flattening of the low energy absorption band and in general, going from a closed ring structure for THT to an open branched chain of TBM, an overall change of the absorption curves. For TBM, an UV absorption spectrum has been reported by Haines et al.,[33] who highlighted a narrower yet more intense band with a maximum absorption of around 215 nm, and a lower energy wider and less intense band at 230 nm.

From this preliminary study, the THT compound appears as the most suitable odorant for the application of the direct UV–Vis absorptiometry. In particular, the low energy absorption having the local maximum at 228 nm does not overlap with the signals due to other components of natural gas, even if its absorption coefficient is 4.8 times lower than that of the main peak.

DOI: 10.1177/0003702820960737

DFT Calculations

Given the scarcity of data in literature and in order to achieve a better comprehension of the nature of the electronic transitions of the odorants, the UV–Vis absorption spectra of TBM and THT have been investigated in details from a computational viewpoint. The UV–Vis absorption spectra are originated from electronic transitions from populated to vacant levels. The excitation may be accompanied by molecular vibrations determined by specific periodic motions of some selected atoms with respect to the others in the molecule. The computational analysis allows to define the nature of both the ground and excited states of the molecule providing useful pieces of information to be compared with the available experimental data. The task is today facilitated by the modern time-dependent DFT methods (TD-DFT).[34] In the present study, the spectroscopic response of molecules such as tert-butyl mercaptan $(CH_3)_3CSH$ (TBM) or tetrahydrothiophene (THT), whose presence is ascertained in the experimental gas mixture, was tested. Therefore, the molecules were firstly fully optimized and spectroscopically investigated, also using various combinations of functional and basis set in order to find the best spectroscopic agreement with the corresponding experimental data. For instance, the three different functionals B3LYP,[35] PBE0,[36,37] and wB97xD,[38] were used in association with either the 6–31+G(d,p) or the DEF2TZVP,[39] with the most satisfactory response observed for the PBE0/6–31+G(d,p) combination. For the sake of simplicity, the first analyzed molecule was TBM molecule, which does not feature any vibronic structure in the experimental UV–Vis spectrum (Figure 1). The computed spectrum exhibits a single peak at 206.8 nm in satisfactory agreement (with ~3 nm of redshift) with the experimental spectrum, featuring a single asymmetric absorption peak at about 204.4 nm (Figure S2, Supplemental Material). Once obtained the satisfactory agreement between the experimental and calculated spectra, we started evaluating the electronic transitions associated with the main peak. The major contributions involve in the descending energy order the HOMO→LUMO+2; HOMO→LUMO+1; HOMO→LUMO transitions with the probability of 12.6, 60.4, and 21.2%, respectively. The MO features of all the involved levels are depicted in Figure 2. In particular, it emerges that the orthogonal and almost pure p_π orbital of the S atom (HOMO) invariably transfers one of its electrons into the vacant S–C and S–H $\sigma*$ level first two transitions, while the third is less crystalline clear). Noteworthy, the electronic transitions of the

DOI: 10.1177/0003702820960737

mercaptan moiety are particularly energetic being the associated wavelength around 200 nm and the calculated energy differences larger than 6 eV.

The electronic transitions for TBM together with their nature were compared with those of simpler correlated compounds that feature a S–H grouping, such as H_2S and MeSH. In no case, the absorption peaks significantly differ from that of TBM at 206.8 nm, given the progressive higher energy shifts (lower wavelengths) in going from TBM to MeSH and H_2S. In particular, the most energetic peak is found for H_2S (203.8 nm), while the shift is almost halved for MeSH (205.4 nm). The results for the three species are summarized in Table I, showing a rather strict similarity of the most important transition.

After these first assessments, the study was addressed to investigate a fourth S-based molecule, namely the tetrahydrothiophene C_4H_8S (THT), which, conversely to the precedent three mercaptan molecules, features a doubly substituted S atom in a cyclic arrangement. Its experimental spectrum significantly differs from the TBM one, both reported in Figure 1, for having a broad peak at 228.6 nm together with a structured one in the 200–210 nm region with a residual shoulder at 197 nm. An initial attempt of reproducing in details the fine structure of the spectrum of Figure 1 by using the standard TD-DFT method failed, because also the calculated spectrum shows a unique peak at 205 nm (Figure S2). In comparison to the previously studied cases, the peak in the simplest computed spectrum for THT corresponds totally to the HOMO→LUMO+2 transition (weight of 96%). The corresponding departure and arrival levels are drawn in Figure S3 (Supplemental Material). In particular, the HOMO is, as in TMB, the p_π sulfur lone pair, with a somewhat reduced weight (from 92% to 86%), while the LUMO+2 is delocalized over the four CH_2 groups of the ring with C–H σ^* character mainly centered at the most distal positions with respect to S. Conversely to the case of the TBM, the electron transition appears to involve C–H σ^* orbitals similarly oriented to the S lone pair. By comparing the pure electronic spectra (Figure S2), a most evident divergence appears in the region 200–215 nm, likely due to neglecting the vibronic components in the performed calculations. For this, we deemed necessary to take into account the Franck–Condon effect,[40] by using the protocol available in the Gaussian 16 package.[41] In this case, the computed UV spectrum of THT was enriched by performing the full optimization of the excited state (still in the singlet), where one electron is actually promoted into the LUMO+2 level. The vibronic structure could be then derived by combining the results of the TD-DFT approach plus those of the excited state optimization. In fact, the final spectrum,

DOI: 10.1177/0003702820960737

shown in Figure 3, exhibits an evident vibronic structure, rather consistent with the experimental one in Figure 1. The reliability of the result is corroborated by the five computed vibronic peaks with almost constant energy separations of ca. 3 nm. The electronic transition is associated with a series of vibrational modes, which are possibly due to the deformation trends of the ring including various C–H vibrations.

UV–Visible Quantitative Analysis of THT and TBM Using Spectra

Spectra was tested at different pressures by plotting the measured THT absorbance values at 230 nm against increasing pressure between 1 and 6 bar (Figure A1a, Appendix). In this pressure range, the instrument showed no deviation from Beer–Lambert law and a reliable sensing of THT with reproducible spectral profiles; the plot, Figure A1 (inset image) exhibits a good fit of data with a value of determination coefficient, R^2, of 99.98% showing the goodness of the linear regression to the set of experimental data up to an absorbance value of 0.2. In practice, a low pressure of 2 bar was chosen for the in-field acquisitions. In a similar way, the relationship between odorant concentration and absorbance was tested at a constant pressure of 2 bar, by plotting the measured THT absorbance values at 230 nm against increasing concentration of THT in methane (Figure A2, Appendix). In the studied concentration range, which is the typical range of concentration of odorant required by law, the signal shows good linearity with a value of R^2 of 99.95%. Once set up for the quantitative analysis, each instrument installed in the pipeline was technically checked and calibrated in situ with odorant/methane canisters at different concentrations and the calibration line was calculated by the automatic system and used as reference. The prototypes were tested in natural gas pipelines in several areas of north Italy in agreement with national natural gas distributors. The aim of the tests was to observe the instrumental response to the variation of odorant concentration, either due to changes in the urban gas demand and/or to system failures. The results discussed in this work are based on the analysis of all the spectra recorded since March 2019 to January 2020 in different pipelines, and their key features are reported below. They might be summarized by dividing the spectra into three classes. The first class of spectra is the overwhelming majority and it consists of those spectra whose absorbance values, recorded in selected wavelengths, show linear relationship with the concentration of sulfur components with acceptable errors. The absorbance measurements were successfully compared to those obtained with standard canisters and,

DOI: 10.1177/0003702820960737

occasionally, the concentrations were also verified by GC with an error, at worst, within ± 10%. Moreover, the absorption profiles do not undergo very large variations in the range of analysis, indicating an overall constant composition of the gas mixture. The second class corresponds to the spectra showing systematic anomalies in the absorption profiles of THT or TBM. These anomalies are present in hundreds of spectra but not in all the pipelines. The analysis of these spectra allowed the identification of some unexpected sulfured pollutants. The third class of spectra groups occasional new profiles of absorption. They are a couple of dozens of cases over thousands of records, and their accidental absorptions are due to pollutants at ppm concentration, mainly due to environmental pollution, or to impurities contained in the commercial odorant or in the upstream charge of natural gas. In this latter class, it is possible to include also those spectra due to some random technical accidents resulting to a sudden variation of the composition of the gaseous mixture; in example we reported the spectra recorded in a pipeline where the odorant injection pump failed (Figure S4, Supplemental Material).

In general, the recorded spectra show the typical absorptions for the THT or TBM, depending on the odorizing agents used in the pipeline, in addition to other components. Two selected groups of spectra recorded with the same experimental conditions in different pipelines are reported in Figure 4.

The spectral profiles reported in Figure 4 show variations of the concentration of THT and some peaks of additional components. In the range 230–235 nm the absorptions are mostly due to THT, endorsing this range as that suitable for the quantitative measurement of THT. The full discernment of the gaseous mixture is quite complex and should be corroborated for each single pipeline, however we have identified the most recurrent components. Firstly, we analyzed the peak at 228 nm which is present in Figure 4. The presence of sulfur based pollutants is plausible and we considered H_2S, MeSH, and Me_2S as possible responsible for the absorptions at 228 nm.[42] The comparative analysis of the spectral data available in literature for H_2S,[20,43] and for Me_2S,[44] ruled out the presence of H_2S and MeSH, leading to the conclusion that the peak at 228 nm might be attributed to the presence of Me_2S with a concentration in the ppm range. As a matter of fact, unexpected traces of Me_2S are occasionally found and tolerated in commercial odorizing agents especially for low cost products; also, blended odorants consisting of 20–30% of Me_2S are commercially available, given its high odorant power and the low cost.[2] Traces of Me_2S may also be found in natural gas even after desulfurization.

DOI: 10.1177/0003702820960737

This hypothesis was corroborated by comparing the spectra of Me_2S, of THT and of the natural gas presumably polluted with Me_2S, in the range 190–280 nm (Figure 5). The plot displays quite a good match for the peaks at 195 nm and at 228 nm, supporting the attribution of these peaks to the adventitious presence of Me_2S.

A careful analysis of the natural gas spectra in Figure 4 highlighted very weak peaks in the range 235–275 nm. A magnification of this range is reported in Figure 6 and it shows a system of peaks apparently due to vibronic structures. The finger-shaped peaks recall the E bands of benzene, with main peaks corresponding to 241, 247, 253, and 259 nm with a large correspondence with the data reported in literature.[45,46] Considering that the two sets of bands of benzene have different molar absorptivity (maximum 256 nm, $\varepsilon = 200$ L* mol^{-1} cm^{-1}; 204 nm, $\varepsilon = 7900$ L* mol^{-1} cm^{-1}; and 184 nm, $\varepsilon = 60000$ L* mol^{-1} cm^{-1}), its presence likely explains some discrepancy of the intensity of the bands observed in figure 4. Actually, an accurate analysis of the peaks at 235–275 nm highlights that it consists of overlapped E bands of different benzene-like structures, with benzene as the largest component.[47,48]

In fact, some of the peaks shown in Figure 6 are slightly shifted with respect to those reported in literature for pure benzene.[45] This fact suggests the likely co-presence of benzene, toluene and xylenes, as confirmed by the measurements with Spectra of standard samples of xylenes, toluene and benzene (Figures S5 and S6, Supplemental Material). It is reasonable to conclude that the peaks system may be attributable to traces of benzene, toluene, and xylenes in the pipeline. The xylenes are the lowest in concentration, and as concerns benzene and toluene their relative concentration was determined by comparing the signals obtained with standard canisters of pure benzene or toluene with those of the natural gas in pipelines as performed for THT and they generally range from 3–12.5 parts per million (ppm) for benzene, and 2.5–10.5 ppm for toluene.

Conclusion

In this work the application of a customized UV spectrophotometer, Spectra, to the detection of THT and TBM in natural gas stream pipelines is presented. First, Spectra was involved in a preliminary study based on in house analyses using THT or TBM canisters in standard conditions to choose an adequate working pressure and to demonstrate the linear relationship between the absorbance and the concentration of the gas. Once the working pressure was chosen

DOI: 10.1177/0003702820960737

and absorbance linearity was proven, Spectra instruments were connected through a direct access to the stream of several urban and non-urban pipelines furnishing spectra all day long. The automatic analysis of the spectra affords to a steady quantitative detection of THT and TBM. Additionally, a detailed computational investigation of the TBM and THT's electronic features was led; the calculations, beside addressing the electronic origin of the spectral results, allowed to determine the wavelength of the maximum absorption for THT and for TBM, with an uncertainty for TBM, which is as small as ≈ 2.4 nm. However, while the quantitative measures of THT performed at 230 nm result to be within an acceptable range of error of ± 10%, the straightforward quantitative measurement of TBM was not possible by direct absorptiometry; in fact, TBM shows the maximum of the absorption in a range of wavelengths where other components absorb, therefore its quantification requires a multiwavelength approach. Interestingly, the analysis of all the spectra herein discussed allows to conceive also further applications for this new device in the field of both environmental sensing and of pipeline's control.

Conflict of Interest

The authors report there are no conflicts of interest.

Funding

This research was partially funded by a research agreement between UNICAM and Automa srl
ORCiD: Rossana Galassi https://orcid.org/0000-0002-8025-9615

Acknowledgments

R.G. is grateful at UNICAM for the financial support of “FAR di Ateneo”, and for the access to the spectroscopy facilities. This research was developed according to a research agreement between UNICAM and Automa srl, which allowed a student to work in this project for her master’s thesis.

Supplemental Material

All supplemental material mentioned in the text is available in the online version of the journal and represents some additional figures of UV spectra recorded by Spectra in addition to

DOI: 10.1177/0003702820960737

graphical depictions of computational calculations.

References

1. W.A.W.A. Bakar, R. Ali. "Natural Gas". 2010. https://www.intechopen.com/books/natural-gas/natural-gas [accessed Aug 5 2020].
2. D. Tenkrat, T. Hlincik, O. Prokes. "Natural Gas Odorization". In: P. Potocnik, editor. Natural Gas. Intechopen, 2010. Chapter 4.
3. J.K. Fink. "Odorization". Petroleum Engineer's Guide to Oil Field Chemicals and Fluids. Boston: Gulf Professional Publishing, 2015. Chap. 15, Pp. 455–475.
4. I. Manisalidis, E. Stavropoulou, A. Stavropoulos, E. Bezirtzoglou. "Environmental and Health Impacts of Air Pollution: A Review". Front. Public Health. 2020. 8(9): Article 14. DOI: 10.3389/fpubh.2020.00014
5. K.M. Van Geem, S.P. Pyl, M.-F. Reyniers, J. Vercammen, J. Beens. "On-Line Analysis of Complex Hydrocarbon Mixtures Using Comprehensive Two-Dimensional Gas Chromatography". J. Chromat. A. 2010. 1217(43): 6623–6633.
6. I.A.A.C. Esteves, G.M.R.P.L. Sousa, R.J.S. Silva, R.P.P.L. Ribeiro, et al. "A Sensitive Method Approach for Chromatographic Analysis of Gas Streams in Separation Processes Based on Columns Packed with an Adsorbent Material". Adv. Mater. Sci. Eng. 2016. Article ID: 3216267.
7. E. Niyonsaba, J.M. Manheim, R. Yerabolu, H.I. Kenttämaa. "Recent Advances in Petroleum Analysis by Mass Spectrometry". Anal. Chem. 2019. 9(1): 156–177.
8. C.D. Pearson. "The Determination of Trace Mercaptans and Sulfides in Natural Gas by a Gas Chromatography–Flame Photometric Detector Technique". J. Chromatogr. Sci. 1976. 14(3): 154–158.
9. J. Kiefer. "Recent Advances in the Characterization of Gaseous and Liquid Fuels by Vibrational Spectroscopy". Energies. 2015. 8(4): 3165–3197.
10. C. McDonagh, C.S. Burke, B.D. MacCraith. "Optical Chemical Sensors". Chem. Rev. 2008. 108(2): 400–422.
11. B.P. Regmi, M. Agah. "Micro Gas Chromatography: An Overview of Critical Components and Their Integration". Anal. Chem. 2018. 90(22): 13133–13150.

DOI: 10.1177/0003702820960737

12. P.E. Leary, B.W. Kammrath, K.J. Lattman, G.L. Beals. "Deploying Portable Gas Chromatography–Mass Spectrometry (GC-MS) to Military Users for the Identification of Toxic Chemical Agents in Theater". Appl. Spectrosc. 2019. 73(8): 841–858.

13. J. de Zeeuw, C. Duvekot, J. Peene, P. Dijkwel, P. Heijnsdijk. "GC: A Review of the State-of-the-Art Column Technologies for the Determination of ppm to ppb Levels of Oxygenated, Sulfur, and Hydrocarbon Impurities in C1–C5 Hydrocarbon Streams". J. Chromatogr. Sci. 2003. 41(10): 535–544.

14. S.-W. Myung, S. Huh, J. Kim, Y. Kim, et al. "Gas Chromatographic–Mass Spectrometric Analysis of Mercaptan Odorants in Liquefied Petroleum Gas and Liquefied Natural Gas". J. Chromatogr. A. 1997. 791(1–2): 367–370.

15. C. Conti, M. Guarino, J. Bacenetti. "Measurements Techniques and Models to Assess Odor Annoyance: A Review". Environ. Int. 2020. 134: 105261–105277.

16. V. Dobrokhotov, A. Larin. "Multisensory Gas Chromatography for Field Analysis of Complex Gaseous Mixtures". ChemEngineering. 2019. 3(1): 13–31.

17. J.J. Davenport, J. Hodgkinson, J.R. Saffell, R.P. Tatam. "A Measurement Strategy for Non-Dispersive Ultra-Violet Detection of Formaldehyde in Indoor Air: Spectral Analysis and Interferent Gases". Appl. Spectrosc. 2019. 73(8): 841–858.

18. B. Trost, J. Stutz, U. Platt. "UV-Absorption Cross Sections of a Series of Monocyclic Aromatic Compounds". Atmos. Environ. 1997. 31(23): 3999–4008.

19. E. Dupuit, A. Dandrieux, P. Kvapil, J. Ollivier, et al. "UV Spectrophotometry for Monitoring Toxic Gases". Analusis. 2000. 28(10): 966–972.

20. F.Z. Chen, W.C.Y.R. Wu. "Temperature-Dependent Photoabsorption Cross Sections in the VUV-UV Region. I. Methane and Ethane". J. Quant. Spectrosc. Radiat. Transfer. 2004. 85(2): 195–209.

21. J.W. Au, G. Cooper, G.R. Burton, T.N. Olney, C.E. Brion. "The Valence Shell Photo-Absorption of the Linear Alkanes, C_nH_{2n+2} (n = 1–8): Absolute Oscillator Strengths (7–220 Ev)". Chem. Phys. 1993. 173(2): 209–239.

22. K. Kameta, N. Kouchi, M. Ukai, Y. Hatano. "Photoabsorption, Photoionization, and Neutral-Dissociation Cross Sections of Simple Hydrocarbons in the Vacuum Ultraviolet Range". J. Electron Spectrosc. Relat. Phenom. 2002. 123(13): 225–238.

DOI: 10.1177/0003702820960737

23. E.A. Fehnel, M. Carmack. "The Ultraviolet Absorption Spectra of Organic Sulfur Compounds. I. Compounds Containing the Sulfide Function". J. Am. Chem. Soc. 1949. 71(1): 84–93.

24. S. Gallot, O. Thomas. "State of the Art for the Examination of UV Spectra of Waters and Wastewaters". Int. J. Environ. Anal. Chem. 1993. 52(1–4): 149–158.

25. O. Thomas, F. Theraulaz, C. Agnel, S. Suryani. "Advanced UV Examination of Wastewater". Environ. Technol. 1996. 17 (3): 251–261.

26. A.J. Blake, J.H. Carver, G.N. Haddad. "Photo-Absorption Cross Sections of Molecular Oxygen Between 1250 Å and 2350 Å". J. Quant. Spectrosc. Radiat. Transfer. 1966. 6(4): 451–459.

27. J.G. Philis, A. Ioannidou, A.A. Christodoulides. "Rydberg States of Styrene from VUV Absorption and REMPI Spectra". J. Mol. Spectrosc. 1995. 174(1): 51–58.

28. B.A. Lombos, P. Sauvageau, C. Sandorfy. "The Electronic Spectra of N-Alkanes". J. Mol. Spectrosc. 1967. 24(1–4): 253–269.

29. G.H. Mount, H.W. Moos. "Photoabsorption Cross Sections of Methane and Ethane, 1380–1600 A, at T Equals 295 K and T Equals 200 K". Astrophys. J. Lett. 1978. 224(1): L35–L38.

30. R. Van Harrevelt. "First Ultraviolet Absorption Band of Methane: An Ab Initio Study". J. Chem. Phys. 2007. 126(20): 204313.

31. G. Herzberg. Molecular Spectra and Molecular Structures. New York: Van Nostrand Reinhold, 1966.

32. D.S. Tarbell, C. Weaver. "The Condensation of Sulfoxides with P-Toluenesulfonamide and Substituted Acetamides". J. Am. Chem. Soc 1941. 63(11): 2939–2942.

33. W.E. Haines, R.V. Helm, C.W. Bailey, J.S. Ball. "Purification and Properties of Ten Organic Sulfur Compounds". J. Phys. Chem. 1954. 58(3): 270–278.

34. E. Runge, E.K.U. Gross. "Density-Functional Theory for Time-Dependent Systems". Phys. Rev. Lett. 1984. 52(12): 997–1000.

35. A. Becke. "Density-Functional Thermochemistry. III. The Role of Exact Exchange". J. Chem. Phys. 1993. 98(7): 5648–5652.

36. C. Lee, W. Yang, R.G. Parr. "Development of the Colle–Salvetti Correlation–Energy Formula into a Functional of the Electron Density". Phys. Rev. B 1988. 37(2): 785–789.

DOI: 10.1177/0003702820960737

37. C. Adamo, V. Barone,". Toward Reliable Density Functional Methods Without Adjustable Parameters: The PBE0 Model". J. Chem. Phys. 1999. 110 (13): 6158–6170.

38. J-D. Chai, M. Head-Gordon. "Systematic Optimization of Long-Range Corrected Hybrid Density Functionals". J. Chem. Phys. 2008. 128(8): 084106–084121.

39. F. Weigend. "Accurate Coulomb-Fitting Basis Sets for H to Rn". Phys. Chem. Chem. Phys. 2006. 8(9): 1057–1065.

40. A. Baiardi, J. Bloino, V. Barone. "General Time Dependent Approach to Vibronic Spectroscopy Including Franck–Condon, Herzberg–Teller, and Duschinsky Effects". J Chem Theory Comput 2013. 9(9): 4097–4115.

41. M.J. Frisch, G.W. Trucks, H.B. Schlegel, G.E. Scuseria, et al. Gaussian 16, Revision C.01. https://gaussian.com/gaussian16/ [accessed 2 September 2020].

42. H. Cui, S.Q. Turn, M.A. Reese. "Removal of Sulfur Compounds from Utility Pipelined Synthetic Natural Gas Using Modified Activated Carbons". Catal. Today. 2009. 139(4): 274–279.

43. W.L. Starr, M. Loewenstein. "Total Absorption Cross Sections of Several Gases of Aeronomic Interest at 584 Å". J. Geophys. Res. 1972. 77(25): 4790–4796.

44. P. Limão-Vieira, S. Eden, P.A. Kendall, N.J. Mason, S.V. Hoffmann. "High Resolution VUV Photo-Absorption Cross-Section for Dimethylsulphide, (CH3)2S". Chem. Phys. Lett. 2002. 366(3–4): 343–349.

45. J. Karwowski. "Assignment of the Electronic Transitions in Benzene". J. Mol. Struct. 1973. 19: 143–166.

46. A. Dawes, N. Pascual, S.V. Hoffmann, N.C. Jones, N.J. Mason. "Vacuum Ultraviolet Photoabsorption Spectroscopy of Crystalline and Amorphous Benzene". Phys. Chem. Chem. Phys. 2017. 19 (40): 27544–27555.

47. M.T. Parsons, I. Sydoryk, A. Lim, T.J. McIntyre, et al. "Real-Time Monitoring of Benzene, Toluene, and P-Xylene in a Photoreaction Chamber with a Tunable Mid-Infrared Laser and Ultraviolet Differential Optical Absorption Spectroscopy". Appl. Opt. 2011. 50(4): A90–A99.

48. W.J. Potts Jr. "Low-Temperature Absorption Spectra of Benzene, Toluene, and Para-Xylene in the Farther Ultraviolet Region". J. Chem. Phys. 1955. 23(1): 73–78.

DOI: 10.1177/0003702820960737

Table I. The most probable electronic transition determined for H_2S, MeSH, and TBM, respectively.

Compound	Transition energy (nm)	Transition energy (f)	Main MO transition	Starting filled MO	Arrival vacant MO
H_2S	203.8	0.0762	HOMO→LUMO	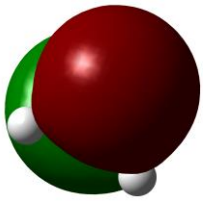	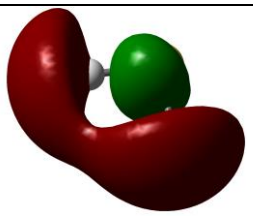
MeSH	205.4	0.0377	HOMO→LUMO+1	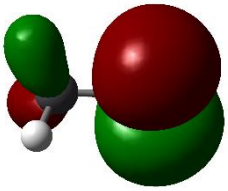	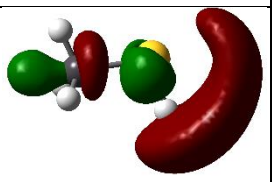
^{t}BuSH	206.8	0.0354	HOMO→LUMO+1	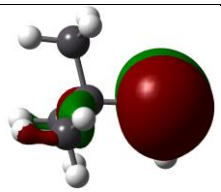	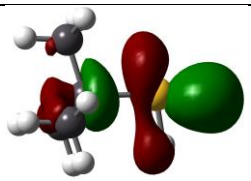

Figures

DOI: 10.1177/0003702820960737

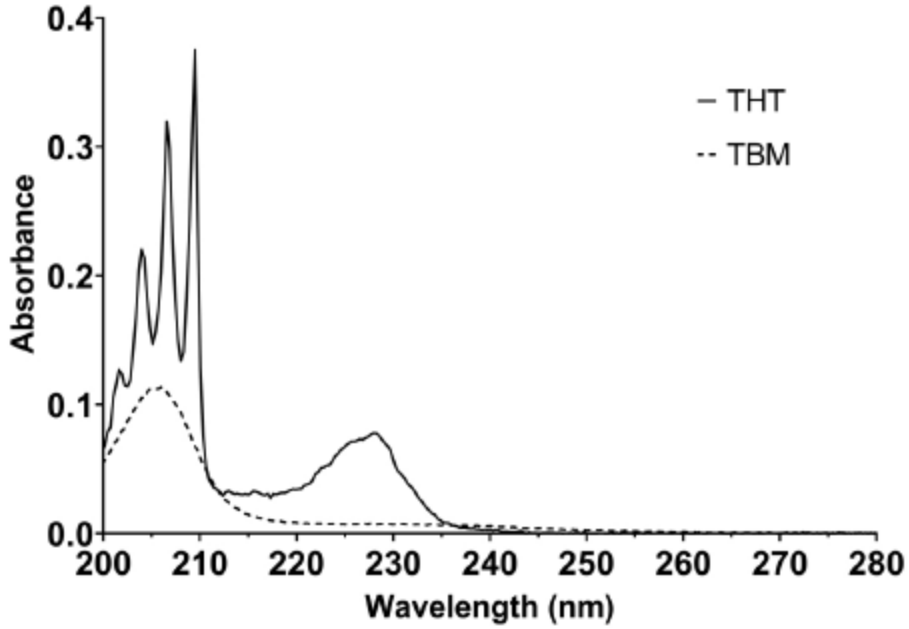

Figure 1. UV–Vis spectra of THT (bold line) and TBM (dashed line) in canister at 46.9 mg/Sm3 and 18.3 mg/Sm3, respectively, in methane (nitrogen as reference gas).

DOI: 10.1177/0003702820960737

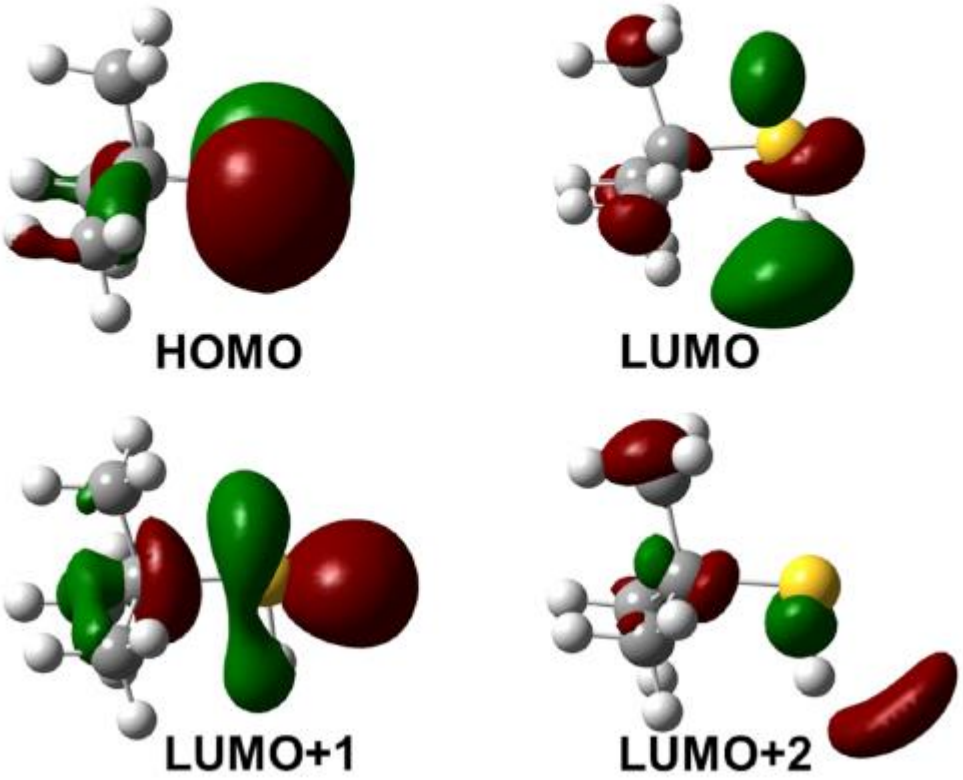

Figure 2. Plots of the molecular orbitals involved in the electronic transitions of the TBM.

DOI: 10.1177/0003702820960737

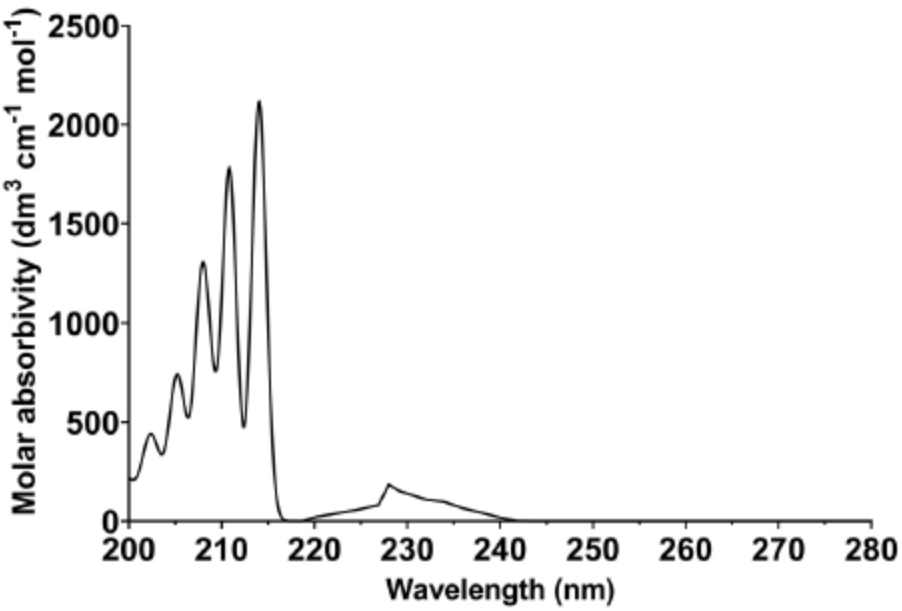

Figure 3. Simulated spectrum for THT in the region between 200–280 nm.

DOI: 10.1177/0003702820960737

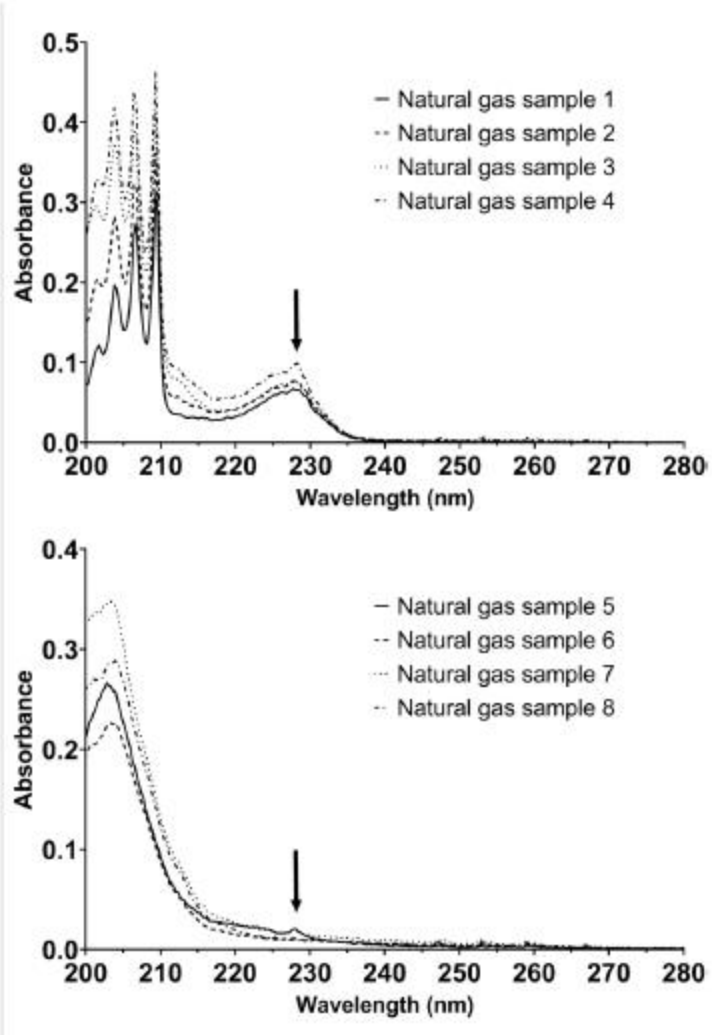

Figure 4. Selected UV–Vis spectra recorded in booths of natural gas stream pipelines odorized with THT (top) or TBM (bottom), attained on different days within May or August 2019, respectively. The spectra show the variation of the odorant content. The arrow labels the adventitious presence of an unusual peak at 228 nm.

DOI: 10.1177/0003702820960737

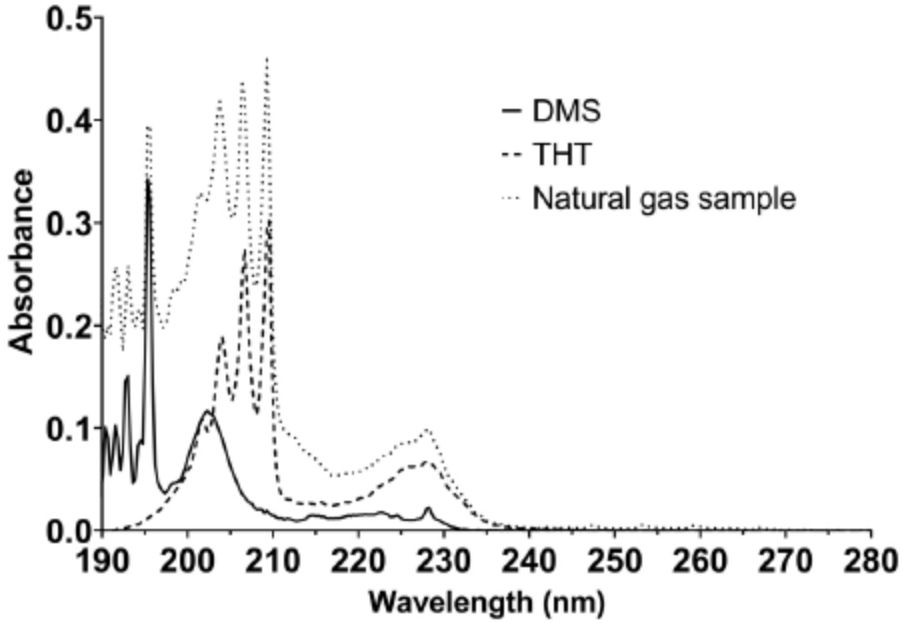

Figure 5. Overlapped spectra of Me2S (taken from literature, bold line), THT (obtained using Spectra, dashed line) and one selected spectrum of odorized natural gas (obtained using Spectra, dotted line).

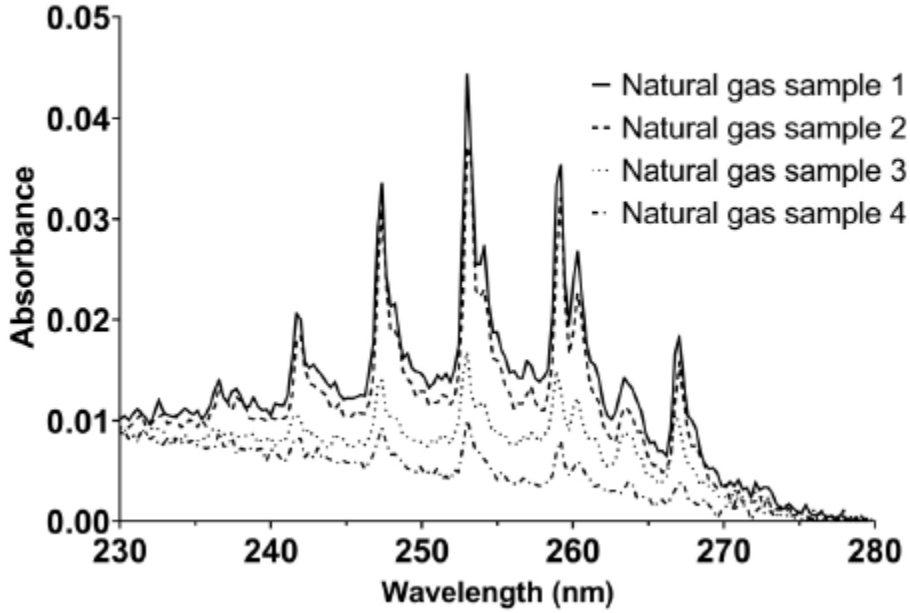

DOI: 10.1177/0003702820960737

Figure 6. Magnification of the 230–280 nm range of selected UV-visible spectra of natural gas streams odorized with TBM shown in Figure 4, highlighting typical bands attributable to benzene analogs.

DOI: 10.1177/0003702820960737

Appendix

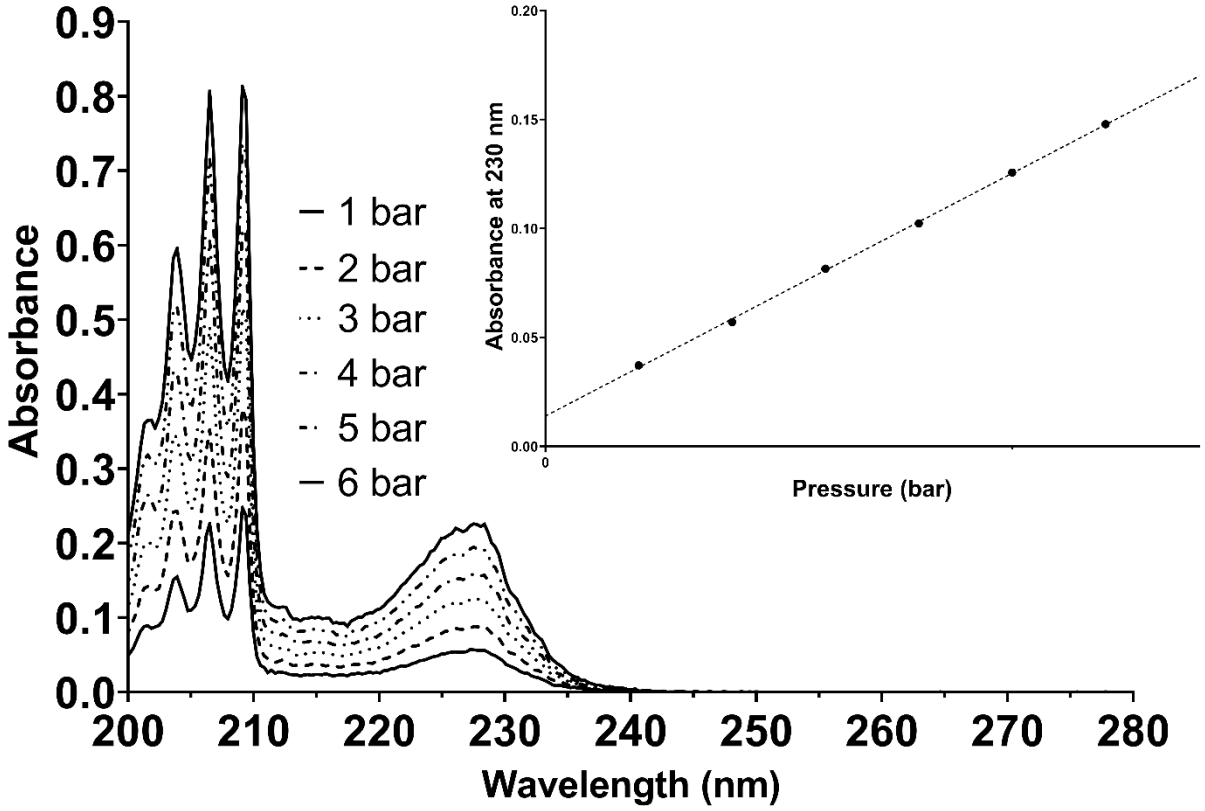

Figure A1. In house measurements of THT in methane canister 54.7 mg/Sm^3 with increasing pressure from 1 to 6 bar, and plot of the absorbance values against the pressure of the gas mixture (inset image).

DOI: 10.1177/0003702820960737

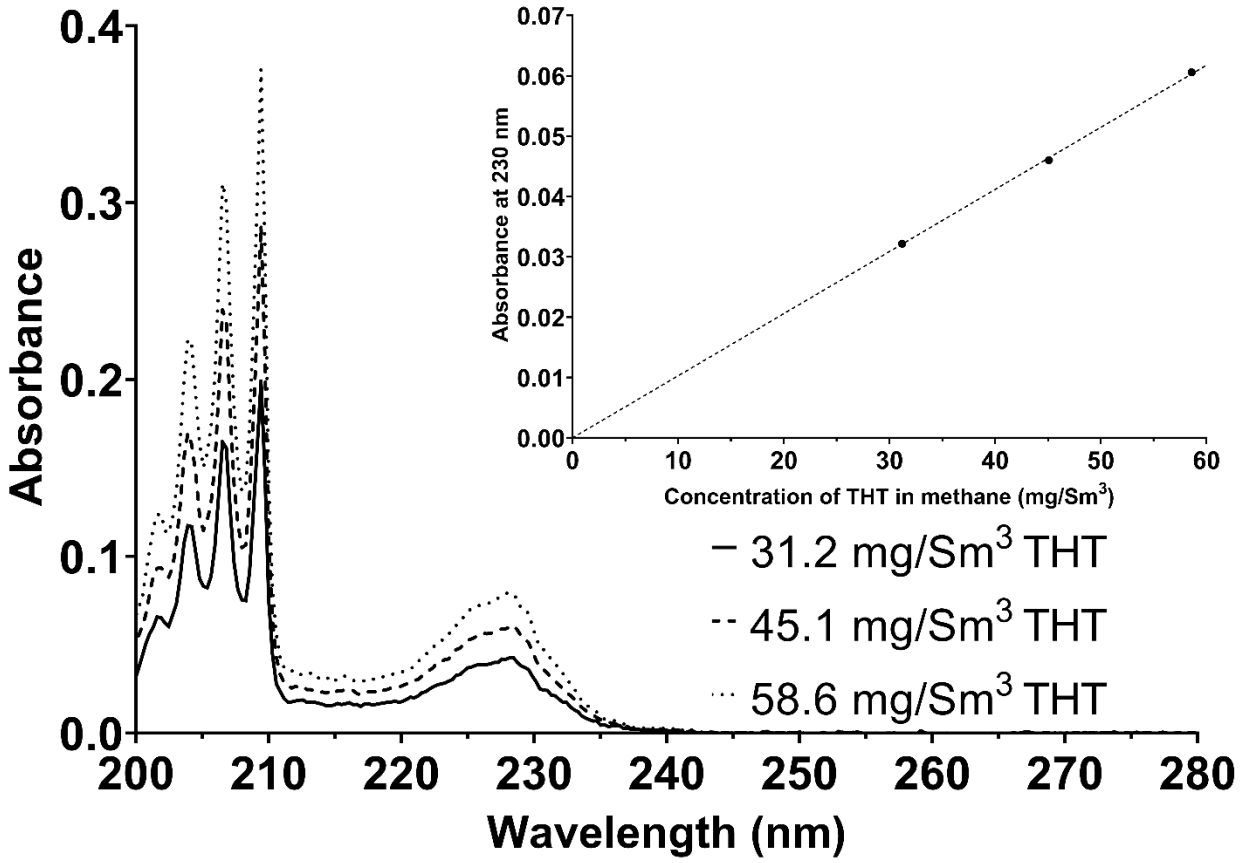

Figure A2. In house measurements of canisters of THT in methane with increasing concentration, and plot of the absorbance values against the concentration of THT (inset image).

Supplemental Material

Odorant Monitoring in Natural Gas Pipelines Using Ultraviolet–Visible Spectroscopy

Rossana Galassi,[1]* Christian Contini,[2] Matteo Pucci,[2] Ennio Gambi,[3] Gabriele Manca[4]

[1]University of Camerino, School of Science and Technology, Chemistry Division, Via Sant'Agostino, 1, Camerino, I-62032, Italy

[2]Automa srl, Via Casine di Paterno 122/A, 60019 Ancona

[3]Università Politecnica delle Marche, Dipartimento di Ingegneria dell'Informazione–Via Brecce Bianche 12, I-60131 Ancona,

DOI: 10.1177/0003702820960737

[4]Istituto di Chimica dei Composti Organo-Metallici, ICCOM-CNR, Via Madonna del Piano 10, I-50019 Sesto Fiorentino, Italy
*Corresponding author email: rossana.galassi@unicam.it

Spectra of Reference Gases: The Case of Air and Polluted Air

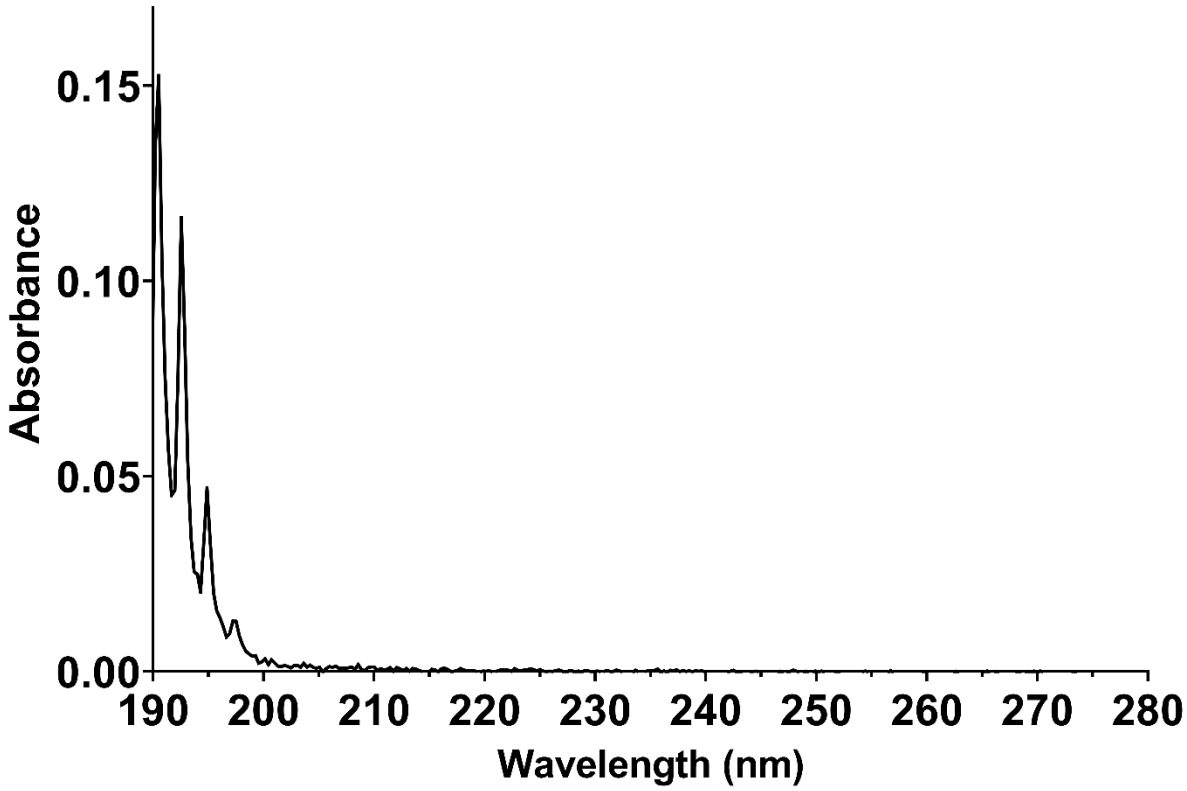

Figure 1S. UV–Vise spectrum of atmospheric air obtained using Spectra in the 190–280 nm range (the blank was acquired on nitrogen).

DOI: 10.1177/0003702820960737

Computational Studies: Simulated Spectra for TBM and THT

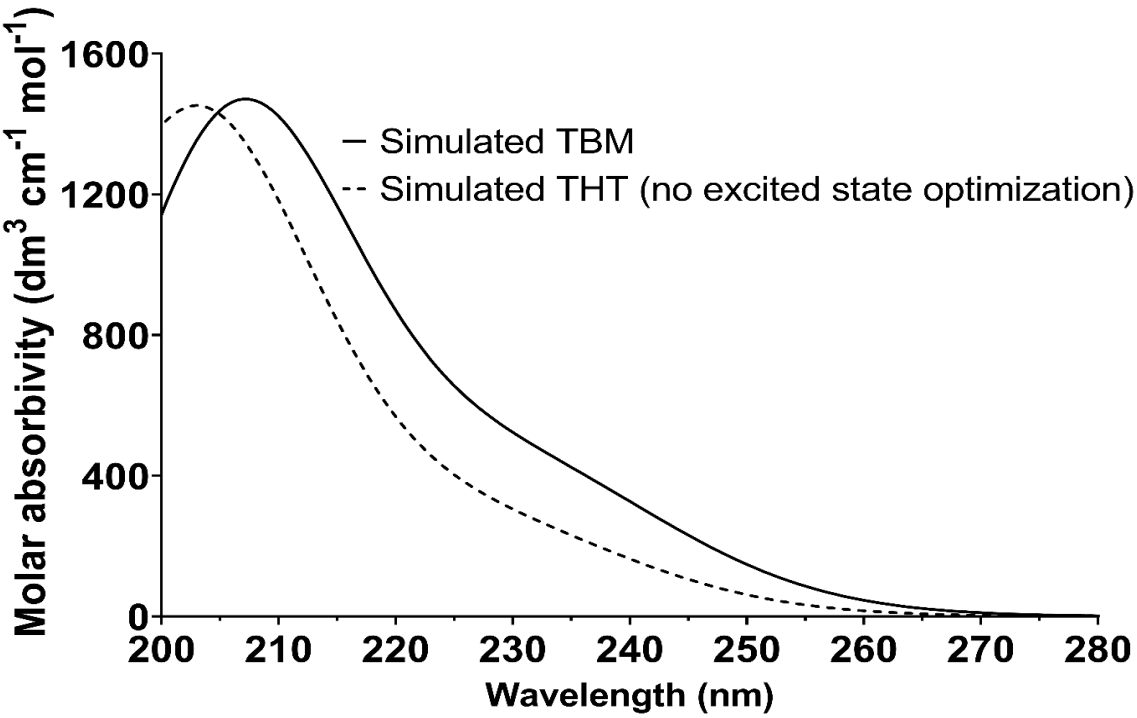

Figure S2. Calculated UV–Vis spectra of TBM and THT without excited state optimization.

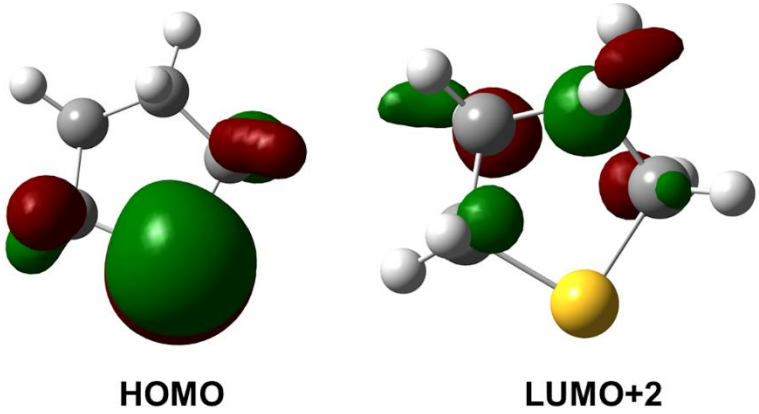

HOMO LUMO+2

Figure S3. Molecular orbitals involved in the electronic transition of THT.

UV–Vis Spectra Obtained Using Spectra.

DOI: 10.1177/0003702820960737

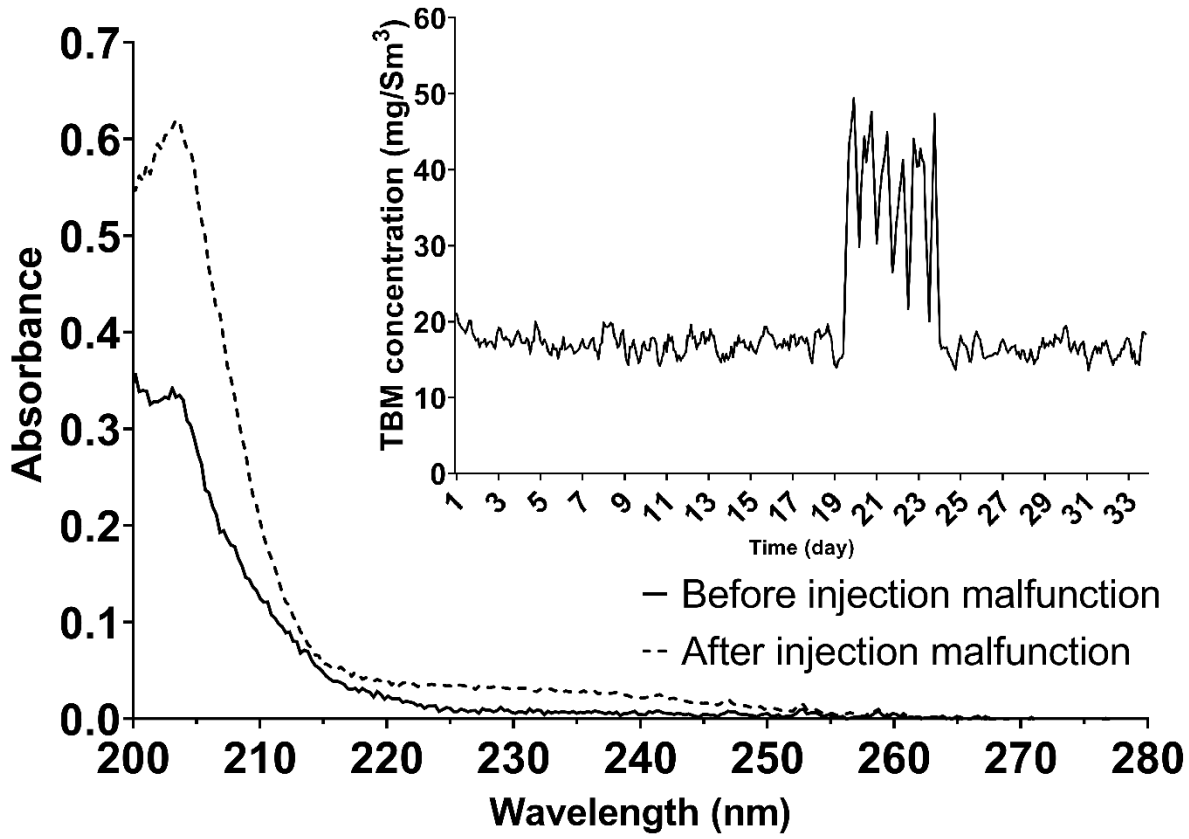

Figure S4. Two selected spectra depicting an abrupt increase of odorant signal due to the malfunction of an injection pump. The inset image shows the measured concentration of odorant over a month of analysis in a booth affected by the malfunction: The increase of odorant levels from days 20 to 24 is notable.

DOI: 10.1177/0003702820960737

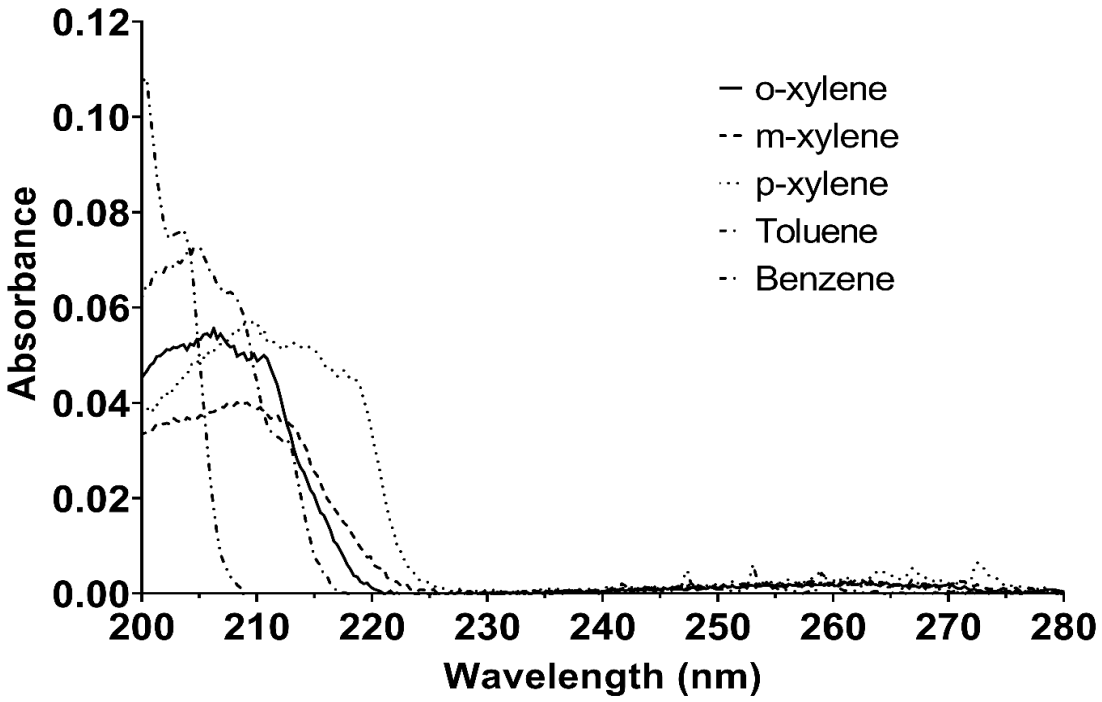

Figure S5. Overlapped UV spectra recorded with canisters of benzene, xylenes and toluene in the range 200–280 nm.

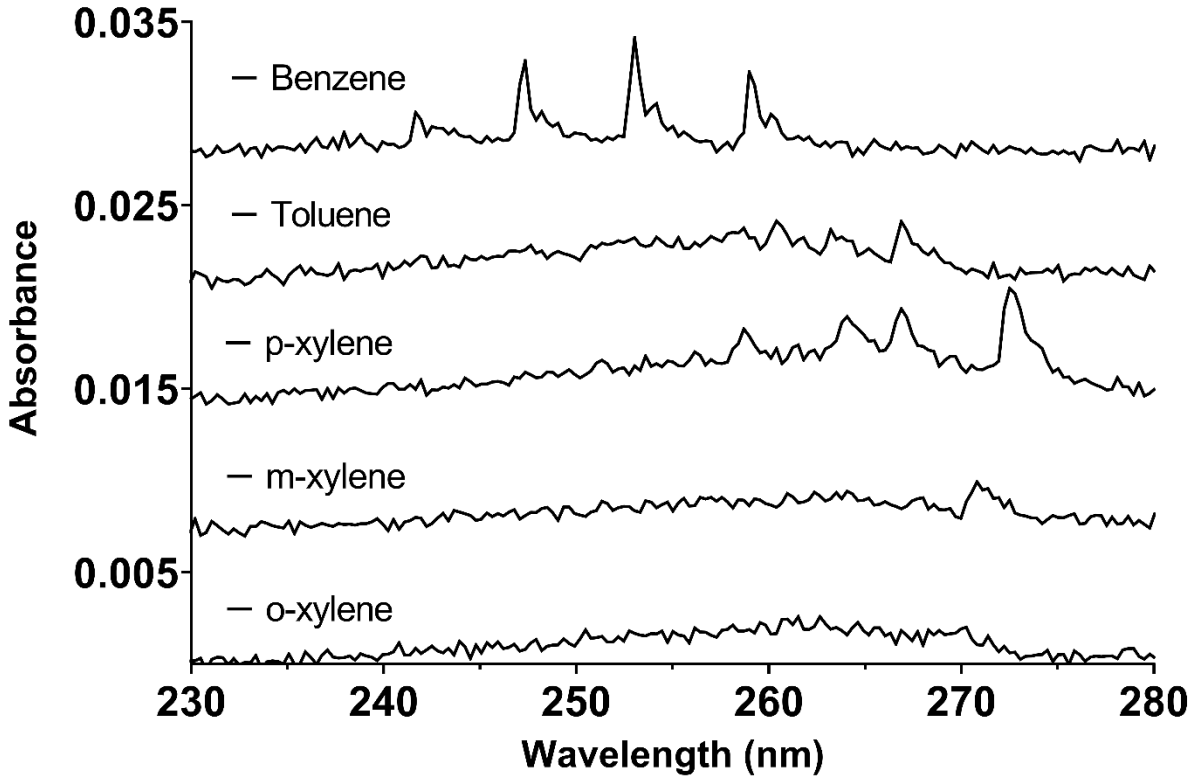

DOI: 10.1177/0003702820960737

Figure S6. UV spectra recorded with canisters of benzene, xylenes, and toluene in the range 230–280 nm (offset between spectra = 0.007).